IPU
DTU Science Park, Diplomvej 376
DK-2800 Kongens. Lyngby

Tel.: +45 45 25 46 00
CVR nr.: 11888933
www.ipu.dk

Optimization of hot gas defrost in industrial refrigeration systems

Prepared for:	Dansk Energi ELFORSK Vodroffsvej 59 1900 Frederiksberg C
PSO project nr.:	347-030
Project period:	2015-2018
Danish title:	Optimering af varmgasafrimning i industrielle køleanlæg

Project consortium

Lars Ove Reinholdt, Jóhannes Kristófersson	Teknologisk Institut
Niels Vestergaard, Morten Juel Skovrup	Danfoss A/S
Alexander Cohr Pachai	Johnson Controls Denmark ApS
Torben Andersen	Danish Crown A/S
Michael Glering	Claus Sørensen A/S
Jorrit Wronski	IPU

Abstract

Industrial refrigeration systems running with ammonia as refrigerant often run with evaporator temperatures below 0 °C. The ice that forms on the evaporator surface is typically removed with a hot gas defrost process. This project investigated two different methods to control the hot gas defrost experimentally and numerically.

The first method, the pressure control method, operates with a fixed evaporator pressure throughout the defrost cycle. It accumulates liquid refrigerant in the beginning of the defrost process and allows gas flow through the evaporator during the whole operating period. The second method is based on draining the evaporator for liquid refrigerant instead. This reduces the initial pressure gradients and minimizes the hot gas consumption upon completion of the ice removal.

An experimental campaign was carried out simulating the operation of a flooded ammonia evaporator and the associated hot gas defrost system. These measurements quantify the differences in energy consumption for the two defrost methods and deliver valuable information for the sizing of defrost systems.

The measured evaporator pressure and mass flow rates were used to validate a dynamic model of the evaporator and the connected valves and pipes. The calibrated model could generate new insights like the impact of the hot gas pressure on the defrost time and the accumulated mass of refrigerant inside the evaporator, which is much lower for the liquid drain method.

The self-adjusting nature of the liquid drain method was found to save 15% of energy per defrost operation compared to a pressure regulated defrost cycle. The savings increase with increasing defrost time since the pressure control method consumes more energy after removal of the ice. For an increased defrost duration of 30 min instead of 20 min, this leads to 30% energy savings for the liquid drain method.

Resume

Industrielle køleanlæg som bruger ammoniak som kølemiddel bliver tit brugt til at levere køling med en fordampertemperatur under 0 °C. Isen, som dannes på fordamperens overflade, bliver typisk fjernet ved hjælp af varmgasafrimning. Dette projekt har eksperimentelt og numerisk undersøgt to forskellige styringsmetoder for varmgasafriming.

Den første metode, trykstyringsmetoden, arbejder med et konstant fordampertryk under afrinmingscyklussen. Denne metode ophober kølemiddel i væskeform i starten af afrimningsprocessen og tillader en gasstrøm igennem fordamperen i hele arbejdsperioden. Den anden metode er baseret på at tappe flydende kølemiddel fra fordamperen i stedet. Dette mindsker trykgradienterne i opstartsfasen og minimerer varmgasforbruget efter isen er smeltet.

En eksperimentel undersøgelse er blevet gennemført, hvor man simulerede driften af en oversvømmet ammoniakfordamper samt det tilhørende varmgasafrimningssystem. Målingerne sætter tal på forskellene vedrørende energiforbrug i forhold til de to styringsmetoder og leverer værdifulde informationer med hensyn til at dimensionere afrimningssystemer.

De målte fordampertryk og kølemiddelflow er blevet brugt til at validere en dynamisk model af fordamperen samt ventiler og rør. Denne kalibrerede model kunne levere ny viden vedrørende indflydelsen af varmgastrykket på afrimningstiden og mængden af kølemiddel i fordamperen, som er meget lavere for den væskebaserede styring.

De selvregulerende egenskaber af væskestyringen har vist energibesparelser på 15% per afrimningscyklus sammenlignet med den trykstyrede afrimning. Besparelserne vokser når afrimningstiden forlænges fordi trykstyringsmetoder bruger mere energi, når isen er blevet fjernet. Når afrimningstiden forlænges til 30 min i stedet for 20 min, ligger energibesparelserne på 30% for den væskebarede styring.

Associated Publications

Vestergaard, N., Kristofersson, J., Skovrup, M. J., Reinholdt, L., Wronski, J., & Pachai, A. (2017). Design requirements for effective ammonia defrost systems. Proceedings of the 7th Conference on Ammonia and CO2 Refrigeration Technologies. Ohrid, Macedonia: International Institute of Refrigeration.

Skovrup, M. J., Wronski, J., Vestergaard, N., Kristófersson, J., Reinholdt, L., & Pachai, A. (2017). Energy Savings Comparing Pressure Controlled and Liquid Drain Controlled Hot Gas Defrost. Proceedings of the 7th Conference on Ammonia and CO2 Refrigeration Technologies. Ohrid, Macedonia: International Institute of Refrigeration.

Kristófersson, J. (2017). Måling af energiforbrug ved varmgasafrimning. DKVF Temamøde “Varmgasafrimning”. Kolding: Dansk Køle- & Varmepumpeforening.

Vestergaard, N. (2017). Varmgasafrimning i industrielle anlæg - metoder og dimensionering. DKVF Temamøde "Varmgasafrimning". Kolding, Denmark: Dansk Køle- & Varmepumpeforening.

Wronski, J. (2017). Energy Savings for Different Defrost Methods. DKVF Temamøde “Varmgasafrimning”. Kolding: Dansk Køle- & Varmepumpeforening.

Kristófersson, J., Reinholdt, L., Vestergaard, N., Skovrup, M. J., Wronski, J., & Pachai, A. (2018). Defrost Efficiency for Ammonia Evaporator Systems. Proceedings of the 13th IIR Gustav Lorentzen Conference on Natural Refrigerants. Valencia, Spain: International Institute of Refrigeration.

Vestergaard, N., & Skovrup, M. J. (2018). Energy and Function Analysis of Hot Gas Defrost. Technical Papers of the 40th Annual Meeting. Colorado Springs, Colorado, USA: International Institute of Ammonia Refrigeration.

Other outcomes

During the course of this project, Danfoss have launched their “Defrost Module” for the “ICF” valve family. The liquid drain based defrost valve station aims at simplifying the installation of and energy efficient defrost cycle for industrial systems. The findings of the project underline the importance of energy-aware defrosting and contributed to estimated savings potential when comparing the new defrost solution to traditional pressure controlled implementations.

Vestergaard, N. (2017). Danfoss White Paper: Effective and cost-efficient hot gas defrost methods - DKRCI.PE.FT0.A1.02. Danfoss.

Contents

1. Introduction

1.1 Motivation and Scope

The evaporation temperature – and thereby the evaporator surface temperature – in refrigeration plants operating below 5-8 °C is below 0 °C. This leads to frost formation on the evaporator surfaces and periodic defrosting is necessary to maintain the cooling capacity. An effective defrost is a key feature of the system to preserve the plant's overall efficiency and product quality. Ideally, all added heat is used to melt the ice on the evaporator surface. The amount of energy used to heat the evaporator coil to temperatures above the freezing point shall be minimized.

Hot-gas defrosting is commonly used in large industrial refrigeration plants and this project investigates the defrost energy consumption of two different control methods and three different evaporator designs. An experimental campaign was designed and conducted to find the governing factors for the energy consumption due to evaporator defrosting. At the same time, a simulation model was developed and eventually validated with the experimental data. The simulation code was then applied to quantify the impact of the different operational parameters. Finally, a system simulation was applied to estimate the energy savings potential for a retrofit solution that modifies the means of hot gas production using a freezing tunnel in an abattoir as example.

1.2 Defrost methods overview

There are numerous different types of defrost systems used in industrial refrigeration, but the most common method is hot gas defrost, which is covered below with its own section. Other methods like electrical defrost, water defrost, etc. are also used in the industry, but are not as widespread and they shall only be discussed briefly here.

Electrical defrost is a simple way to remove ice from evaporator surfaces and is based on the ohmic heating of the evaporator. Electrical defrosting is normally built as an "external" system, which does not interact with the refrigerant in the system. It is relatively inexpensive to install and can be used as retrofit solution. However, it also requires a significant amount of energy and is mostly limited to smaller, less advanced systems. For low temperature operation and systems with high defrosting sequences, electrical defrosting is not used very often, due to the high operating costs.

Water-based defrost is also an inexpensive way to remove ice where sufficiently warm water runs over the ice-covered surface initiating thawing and the removal of ice pieces. Its major disadvantages are related to water consumption and water handling to avoid spillage and overflow. Furthermore, this method is not applicable for systems operating at low temperatures. This system can also be classified as an "external" system as it is not integrated with the refrigeration system.

Reverse cycle defrost makes the whole refrigeration system to run "backwards" and thus requires a unique system design. It is not very widespread, but it has traditionally been used in low pressure receiver systems in the UK only. Such a defrost system can operate very fast and efficient, but due to the lack of experience and references, it is not very common outside of the UK.

Natural defrost in industrial systems relies on the environment to provide the thermal energy needed to remove the ice on the evaporator. It is thus typically used in countries with hot climate, and in systems where it is possible to separate the evaporator from the cooling demand and to connect it to outdoor air, e.g. Penthouse evaporators in cold stores. This

method is simple and energy efficient but is usually rather slow and cannot be applied in closed locations, which makes it a niece design for industrial applications.

Hot gas defrost is the most common method for defrosting industrial evaporators. By reversing the flow of refrigerant in a single evaporator, the thermal energy from the compressor discharge gas can be exploited to heat the evaporator eventually melting ice and evaporating remaining droplets. Two different methods are used to control the defrosting process: pressure control (PC) and liquid drain (LD), both of which will be covered in more detail below.

1.3 Hot gas defrost systems

Defrosting with hot gas is known to be a relatively fast and effective method to remove ice from evaporator surfaces. Compared to the other methods mentioned above, it also has a good energy efficiency, which makes it a popular choice for industrial refrigeration systems. However, hot gas defrost systems have to be designed correctly, in order to obtain the expected performance. Experience shows that there are several pitfalls, which can lead to ineffectiveness, and, in the worst case, increase the risk of serious accidents due to inappropriate design and incorrect operation.

Fast and effective defrosting has the highest priority for almost all applications. In order to fulfil this requirement, the system needs to be designed and controlled correctly including properly sized piping and valves. A common system design is presented in Figure 1.

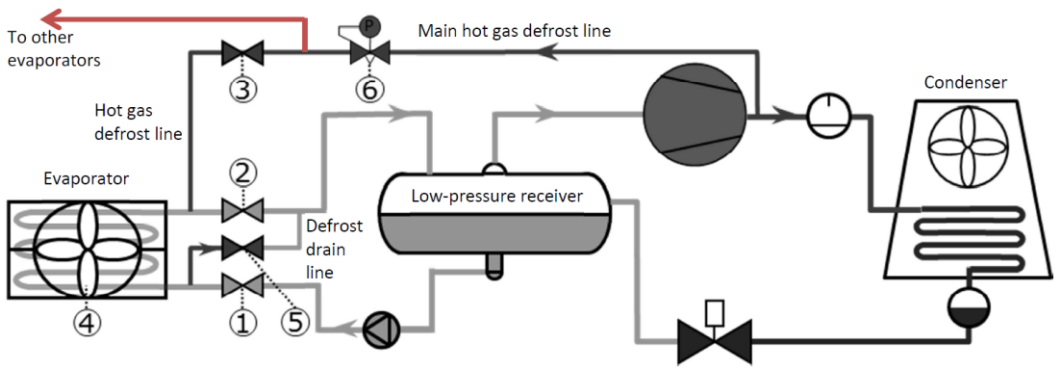

Figure 1: Hot gas defrost principle in an industrial overfeed system

During normal operation, the discharge gas from the compressor is cooled and condensed in a condenser, while during defrost, a part of the discharge gas is directed through valves 6 and 3 and injected into the evaporator that should be defrosted. Valve 6 is used to reduce the hot gas pressure so that the evaporator does not experience extreme pressure variations when connecting it to the discharge line upon opening of valve 3. Common industrial systems can operate with ammonia saturation temperatures from -45 °C to +45 °C, which correspond to system pressures in the range of 0.5 bar to 20 bar. After initial pressure equilibration, the evaporator is acting as a condenser and the condensate is directed through valve 5 to the low-pressure receiver. All liquid is separated in the receiver and pumped to the evaporators operating in cooling mode. The flash gas and non-condensed blow-by gas passing through the evaporator have to be recompressed, which causes the major part of the energy consumption associated with defrost cycles. The losses caused by the blow-by gas depend on how valve 5 is controlled. The PC method can create significant losses, whereas the losses for the LD method tend to be much smaller. Both methods are explained in detail later.

1.4 Hot gas defrost cycle example

A typical defrost cycle consists of different phases that define the transition from normal operation to defrost operation and back to normal operation. The gradual changes in temperature and pressure reduce mechanical loads and thus avoid the formation of leakages and extend the evaporators lifetime. An overview of a typical defrost operation sequence is presented in Figure 2.

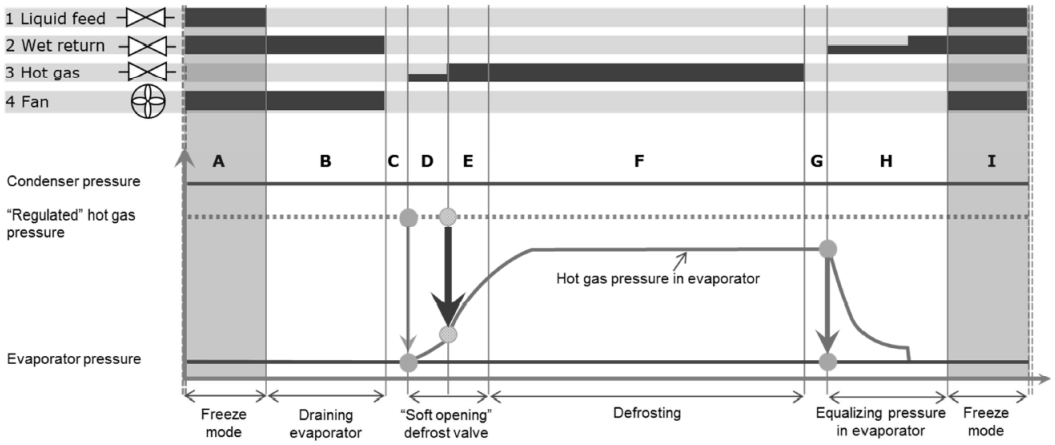

Figure 2: Example of a hot gas defrost sequence

The different components that have to be controlled are numbered from 1 to 4 in Figure 2 and the numbers correspond to the numbers used in Figure 1. A description of the different phases can be found below:

A. Freeze mode: normal operation
B. Draining: Close liquid feed line 1 and wait for remaining refrigerant to evaporate
C. Stabilizing: Close valve in wet return line 2, stop fan 4, wait for conditions to settle
D. Soft opening step 1: Open hot gas supply valve 3 a little bit
E. Soft opening step 2: Open hot gas supply valve 3 fully
F. Defrosting: Heat up evaporator and remove ice while draining through valve 5
G. Stabilizing: Close hot gas supply valve 3, wait for conditions to settle
H. Equalizing: Gradually open wet return line, let pressure drop to operating conditions
I. Freeze mode: Open liquid feed line 1, start fan 4

The described defrosting sequence is based on the recommendations for safe operation put forward by the International Institute of Ammonia Refrigeration (IIAR). Other sequences and methods may also fulfil these requirements. The main principle is that the has to be emptied by evaporating the remaining liquid, before injecting hot gas to ensure a safe operation. After the defrosting has been completed, the evaporator needs to be brought back to freezing mode. Depending of the defrosting process, controlling method and defrosting time, the evaporator may still contain some liquid. It is important to ensure a prober equalizing to the evaporating pressure, in order to avoid pressure shocks and liquid hammer effects.

Some operators decide to minimize defrosting time and apply a forced drain method. This modified sequence skips phase “B” partly or completely “pushing” the remaining liquid out of the evaporator by opening valves 3 and 5 almost simultaneously. This method has to be applied carefully due to the risks associated with it. The IIAR does not recommend such operation.

1.5 Control of hot gas defrost systems

The hot gas flow rate has to be controlled during the defrost cycle to maintain a high pressure and a high condensation temperature inside the evaporator should be heated. The two designs investigated here are the pressure control and the liquid drain method. Both principles are sketched in Figure 3.

The pressure control method uses a valve to control the upstream pressure in the drain line. This is a reliable and simple system. Despite its popularity, this method can consume significant amounts of energy, if the defrost cycle is terminated too late. The liquid drain method on the other hand minimizes the refrigerant flow by adapting the line pressure to maximize the production of liquid refrigerant and thus exploiting the phase change of the supplied hot gas.

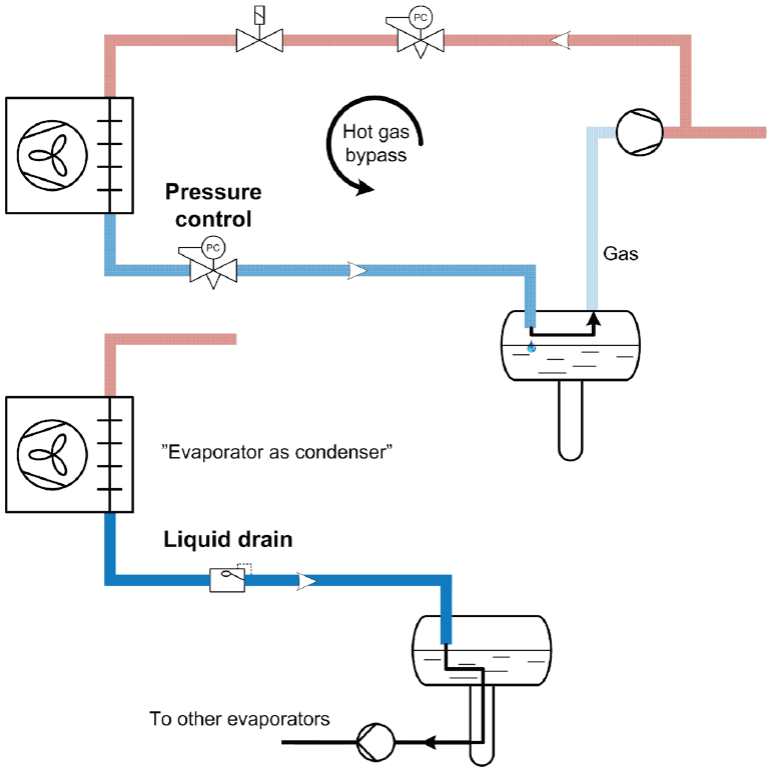

Figure 3: Pressure Control and Liquid Drain Control of Defrost Cycles

While the pressure control method allows refrigerant to pass through the defrost lines based on the set point for the pressure. This leads to shorter contact times at the interface between the refrigerant and the evaporator wall reducing the heat exchange. The liquid drain method on the other hand requires a certain amount of liquid to open the main drain line valve while a small bleed valve can be used to stabilized operation and to remove flash gas that may form upstream of the valve. A correctly sized bleed valve only allows a fraction of the gas flow to bypass the evaporator compared to the pressure control method.

1.6 Energy savings potential

The reduced hot gas consumption for the liquid drain method is the key for the energy savings potential associated with this method. The mass flow rates sketched in Figure 4 can be used to explain the differences between the PC and the LP method. The figure is a simplified version of the data presented in (Vestergaard & Mikhailov, Analysis of various ammonia defrosting systems, 2016).

The low pressure in the evaporator at the beginning of the defrost cycle causes a very high initial hot gas mass flow rate that is only limited by the flow resistances. After some time, the pressure stabilizes slightly above the melting temperature of the ice on the evaporator and the actual defrost operation is carried out. As soon as the ice has melted, the temperature of the evaporator increases. During this phase, the pressure-controlled mass flow rate remains constant while the mass flow rate for the liquid drain methods drops as it follows the condensate production rate.

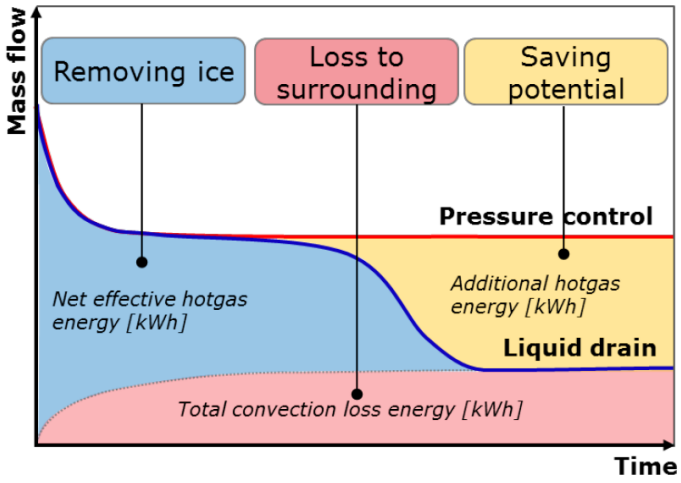

Figure 4: Energy distribution for a hot gas defrost cycle

The coloured areas in Figure 4 relate to the compression energy needed to provide the consumed hot gas. It is further assumed that this energy correlates with the amount of energy supplied to the evaporator. The different contributions to the total energy consumption are:

- Net effective hot gas energy: This is the amount of energy that is used to heat the evaporator and to melt the ice on the surface (blue area).
- Total convection loss: This is the amount of energy that is transferred into the surroundings of the evaporator (red area).
- Additional hot gas energy: This is the difference in energy consumption between the two control methods (yellow area).

The figure also illustrates that there is a lower limit for the energy consumption that is governed by the heat transfer to the environment. This heat transfer occurs due to the temperature difference between the evaporator and the cold room and cannot be avoided.

Besides the control methods, the hot gas production itself also has an energy savings potential. Many plants run with a relatively high minimum condensing temperature to get a high temperature and pressure of the hot gas used for defrosting. This leads to unnecessary energy consumption since the air temperature in Denmark in most part of the year is low enough to decrease the condensing pressure further. Having a dedicated compressor for hot gas production can lead to significant energy savings and help to reduce the electricity consumption of the plant and eventually increase the COP. By introducing a serial compressor in the hot gas line, it may be possible to compress only the part of mass flow that is used for hot gas defrosting and thus optimize the system by decoupling the condensing pressure of the plant and the defrost method.

2. Experimental campaign

2.1 Test rig and components

The measurements described in this project are carried out by the Danish Technological Institute in their test facilities in Århus, Denmark. For more details, the reader is referred to (Kristófersson, et al., 2018). In brief, the system setup resembles an industrial installation with a recirculation pump. The evaporator of the ammonia refrigeration plant is placed in a climate chamber with controllable humidity and temperature to simulate different operating conditions. The water mass balance during icing and defrost operation is used to monitor the defrost performance and to track the completion of the ice removal. A sketch of the installed valves and the piping layout can be found in Figure 5. The tests typically start with adding approximately 50 kg of ice to the evaporator during about 60 h of operation at high relative humidity levels.

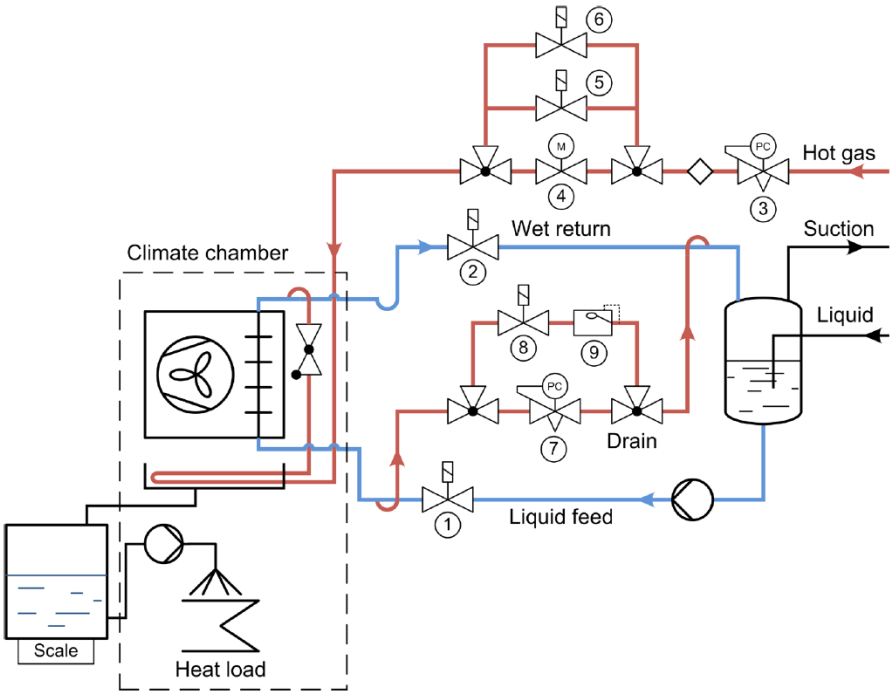

Figure 5: Layout of the defrost test rig

The hot gas entering the defrost line has a pressure of 12 bar that matches a condensing temperature of 31 °C which is reduced to 7.3 bar matching a 15 °C saturation temperature using valve 3.

Figure 2 describes a so called “soft opening” of the hot gas supply at the beginning of the defrost cycle. The test setup implements this with either a combination of small hot gas valve 6 that is opened before the main hot gas supply valve 5 is activated or with a gradually opening motor valve 4.

Different evaporator models are tested and experiments have been conducted with a bottom-feed evaporator, a top feed configuration as well as a side feed design. As also shown in Figure 6, the designs that are popular in the US (top feed and side feed) are equipped with distribution nozzles that create an additional pressure drop whereas the European bottom feed layout does not have such features. More details regarding the evaporator layout can be found in

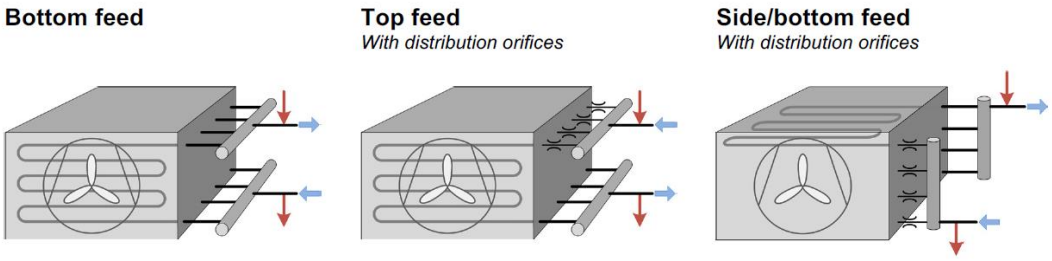

Figure 6: Different evaporator configurations

In the return line, pressure can be controlled with valve 7 to stay at 5.6 bar equal to a saturation temperature of 7.3 °C. Alternatively, solenoid valve 8 can activate the liquid drain valve 9 that is equipped with a small gas bypass allowing the pressure as a free variable.

2.2 Measurement results

To identify differences in the defrost performance of the three evaporator types, a visual inspection of the ice layer on the evaporator was carried out. Figure 7 shows pictures of the different evaporator types at selected stages of the defrost cycle. The pictures were taken at the beginning of the defrost tests and at approximately 25%, 50% and 75% of the defrost cycle as well as at the end.

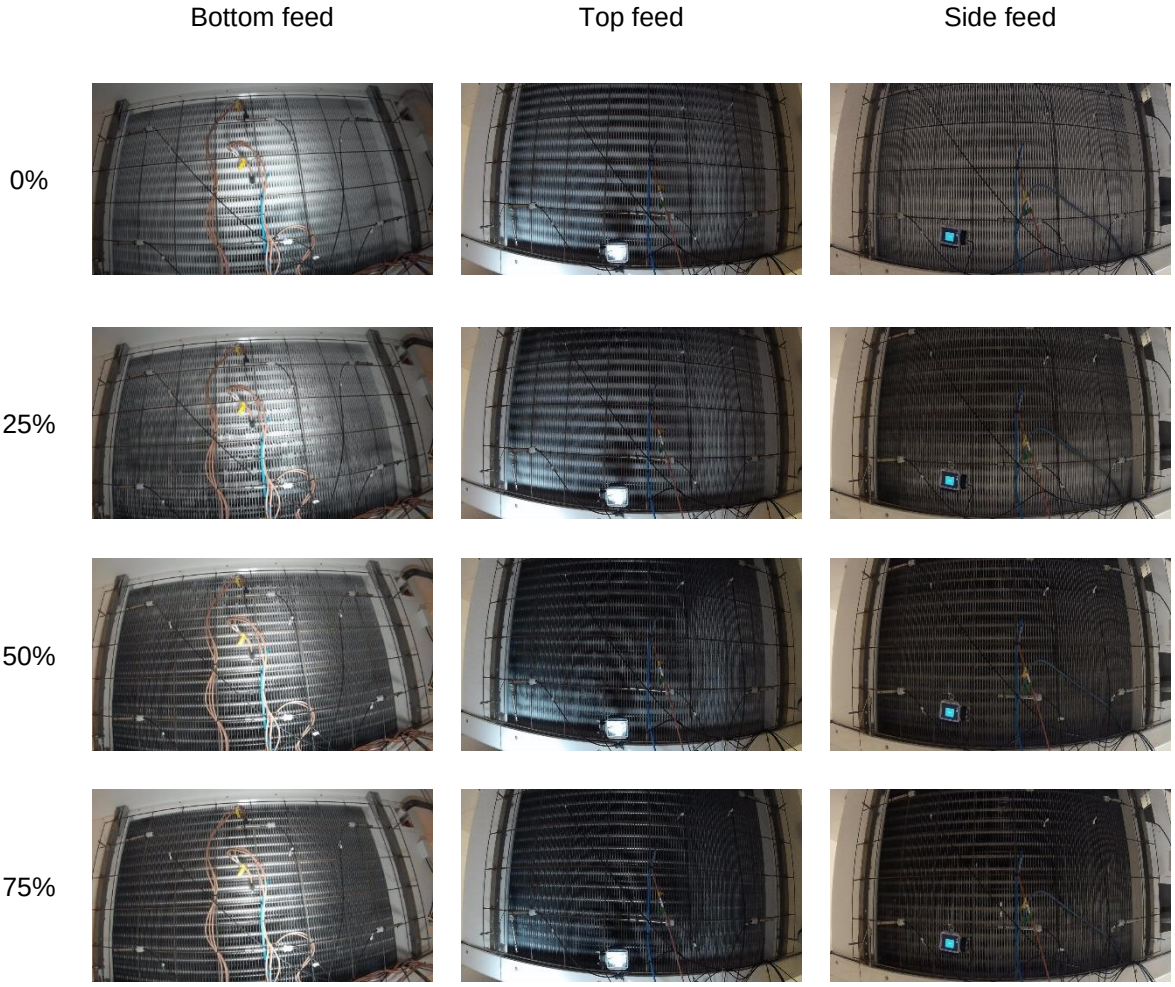

100%

Figure 7: Progressing defrost of different evaporator types

The bottom feed and the top feed type devices exhibited a uniform ice removal that started at the hot gas inlet. The ice was removed gradually and the cleaned area grew continuously until all ice was removed. The defrost of the side feed units, however, did not progress as a uniform front and refreezing of dripping water occurred at several places on the lower side of the unit.

The hot gas mass flow rates during defrost are depicted in Figure 8 for different control methods and evaporator types. The defrost cycle started with a sharp initial increase of the mass flow rates approximately 10 min after the data recording was initiated.

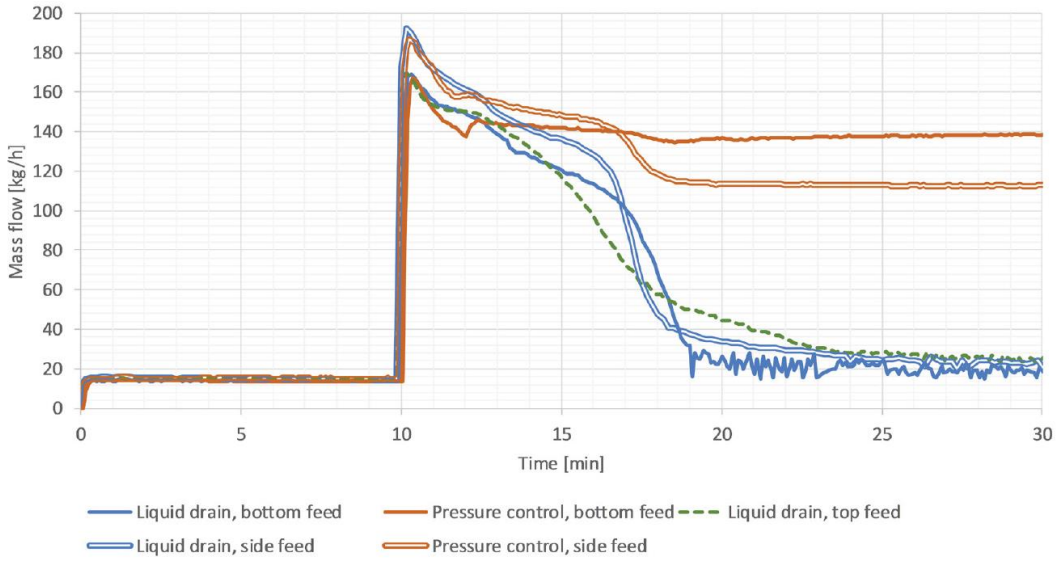

Figure 8: Hot gas mass flow rates for different evaporator types end control methods

During the first minutes of the measurements, all hot gas is condensed and the mass flow rates for PC and LD operation are similar. After approximately 150 s, the mass flow rates for the LD method start to decrease while the PC measurements continue to operate with a high throughput. A second and more pronounced drop in mass flow rates occurs around 8 min after defrost start. At this time, the hot gas condensation rate is assumed to decrease causing the LD device to close leading to an increase of the pressure inside the evaporator. The PC measurements for the side feed unit also exhibit a similar behaviour and here the assumption is that the decrease in average density at the evaporator outlet leads to highe pressure drops at the distribution nozzles. The PC measurements for the bottom feed unit are almost constant which may be related to the absence os the distribution orifices.

The distribution nozzles of the top feed unit are located at the hot gas inlet while they are located at the drain connector for the defrost cycle in the side feed unit. This means that the nozzles of the top feed unit throttle a low density flow regardless of the condensation rate inside the evaporator. The lower mass flow rate figures for the top feed design support his interpretation. The mass flow profile has a less distinct shape and the defrost operation seems to take longer for this unit.

The mass of water that returned from the tested evaporator is used as a measure for the progression of the defrost cycle. The sum curves for the return water are shown in Figure 9 and the inclination of the curves can be inyterpreted as the melting rate of the ice on the evaporator.

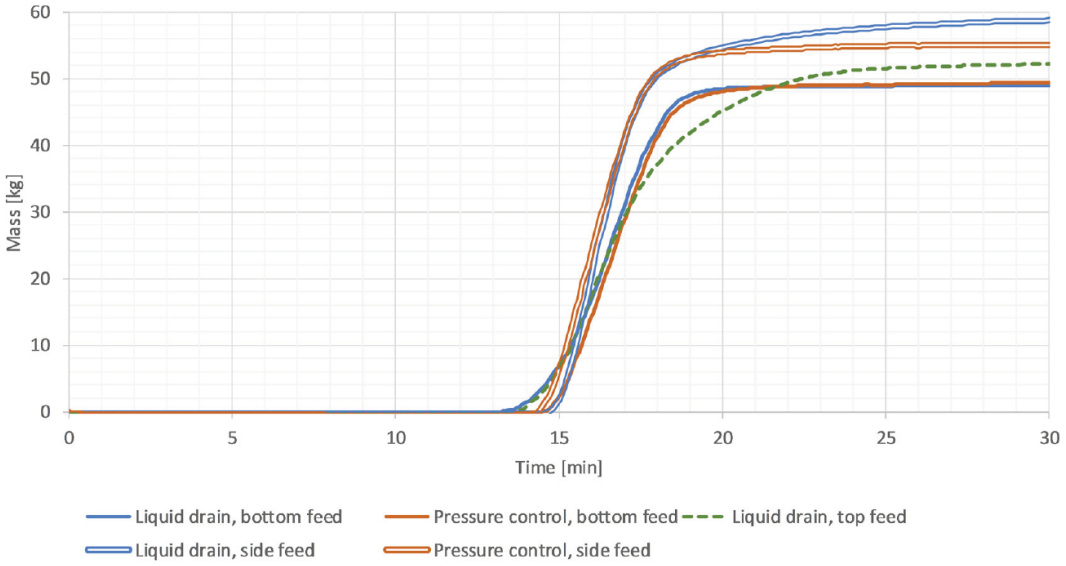

Figure 9: Collected water for the different evaporator types and control methods

Using the return water measurements, the initial phase of high mass flow rates in Figure 8 can be identified as heating of the evaporator and the ice layer since there is no water flow in Figure 9 before approximately 3 min after defrost start.As soon as the melting temperature of the ice is reached, liquid water is produced at a contant rate until all ice has been removed and the mass of the returned water remains constant.

The decreased defrost rate for the top feed unit mentioned above can be verified with the water measurements that reveal a smoother transition at the end of the defrost cycle. This also affects the defrost time and the ice on the top feed evaporator seems to disappear slower than on the other units.

3. Simulations

3.1 Model description

A dynamic simulation model was developed to identify additional operating conditions and to extract information that is difficult to measure. The model focusses on the hot gas line including valves and the evaporator. The actual components are shown in Figure 10 and the valve-like flow resistances in the inlet and outlet pipe of the evaporator are used to include flow losses from piping and fittings. The general design of the model is a simplified version of the test setup shown in Figure 5.

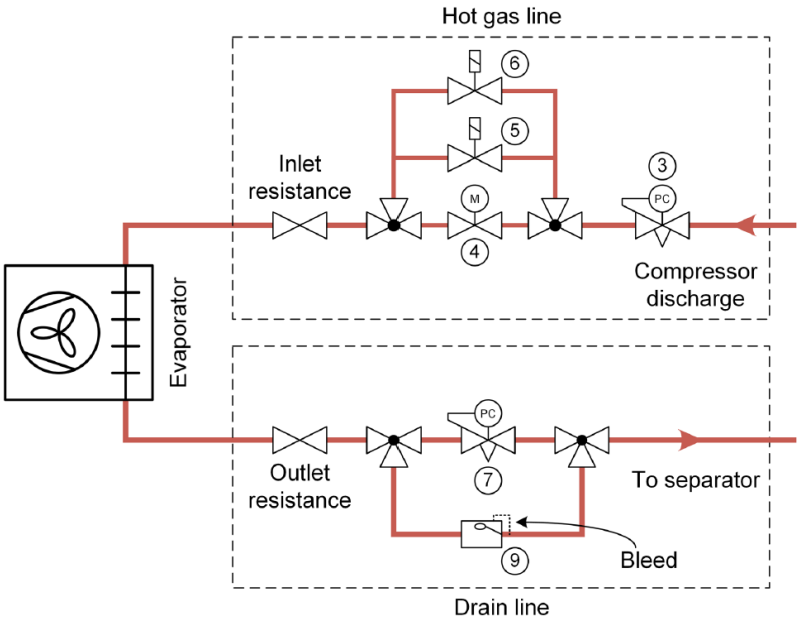

Figure 10: Overview of the simulation model

A detailed description of the model can be found in (Skovrup, et al., 2017), but a couple of key properties shall be repeated here.

The valves in the hot gas and in the drain line are modelled using the equations from EN 60534-2, assuming that the expansion factor for additional flow losses due to density changes is set to unity

$$\dot{m}_{valve} = N \cdot K_{v,valve} \cdot \sqrt{\rho_{valve,inlet} \cdot \left(p_{valve,inlet} - p_{valve,outlet}\right)} \quad (1)$$

and with N being a constant for unit conversions. The different valves for PC and LD are assumed to work ideally, which means that they will allow all liquid to leave the evaporator as long as the maximum flow rate is not reached. For the LD valve lets all liquid escape while the bleed flow adds a certain portion of gas to the mass leaving the system. The gaseous outlet is either regarded as saturated flow or superheated flow depending on whether liquid is present or not.

The evaporator itself is modelled as a lumped volume with thermal mass stored in the wall and in the ice on the evaporator. Evaporator geometry is not included in the model and the reduced layer model is shown in Figure 11.

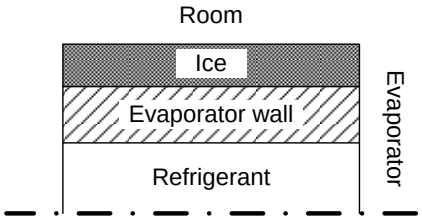

Figure 11: Evaporator model layers

The absence of geometrical features makes it necessary to include the flow resistances is the different evaporator types as part of the inlet and outlet resistances.

To accommodate the dynamic behaviour of the system, the model is built with four states that control which set of equations is active at a certain point in time. Furthermore, the states described below also reset the solver allowing it to handle discontinuities more efficiently.

1. Filling of evaporator, either by soft-gas solenoid or slow-opening motor valve. An initial pressure equilibration that handles flow at large pressure gradients.
2. Heating of ice, where the initial temperature of the ice and the wall increases to 0 °C. No phase change occurs on the outside of the evaporator.
3. Melting of ice until the mass of ice on evaporator reaches 0 kg. No temperature change occurs in the ice layer.
4. Heating of room, where all ice has been removed and heat is just added to the room. Continues until defrost ends.

Note that state 1 is related to the flow conditions, while the other states take care of the heat transfer. Due to the above, state 1 is independent from the other states and can be active together with any of the other states.

3.2 Validation of simulation results

Focussing on the bottom feed evaporator, the model has been validated for PC and LD operation using the pressure and mass flow rates shown in Figure 12 and Figure 13, respectively. Note that state 1 overwrites that other states while it is active and that state 2 runs in parallel with state 1 in the beginning of the simulation.

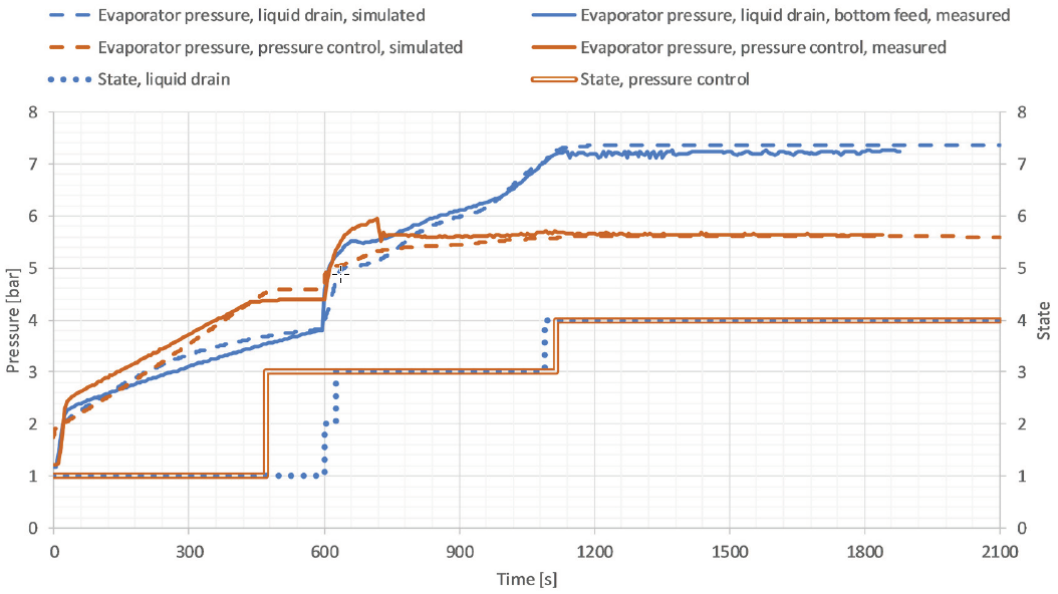

Figure 12: Measured and simulated evaporator pressure

The curves shown in Figure 12 show that the pressure in the simulated evaporator matches the experiments. However, there are differences at the beginning of the filling phase as well as during the highly dynamic period after the opening of the main defrost valve at 600 s after defrost start.

The initial pressure build-up is slower for the LD method since the drain valve opens as soon as liquid is present, while the pressure control valve only opens according to the upstream pressure. During the defrost, the condensation rate of refrigerant inside the evaporator drops and the LD method reacts with a reduced the mass flow rate and an increasing pressure until it reaches inlet conditions.

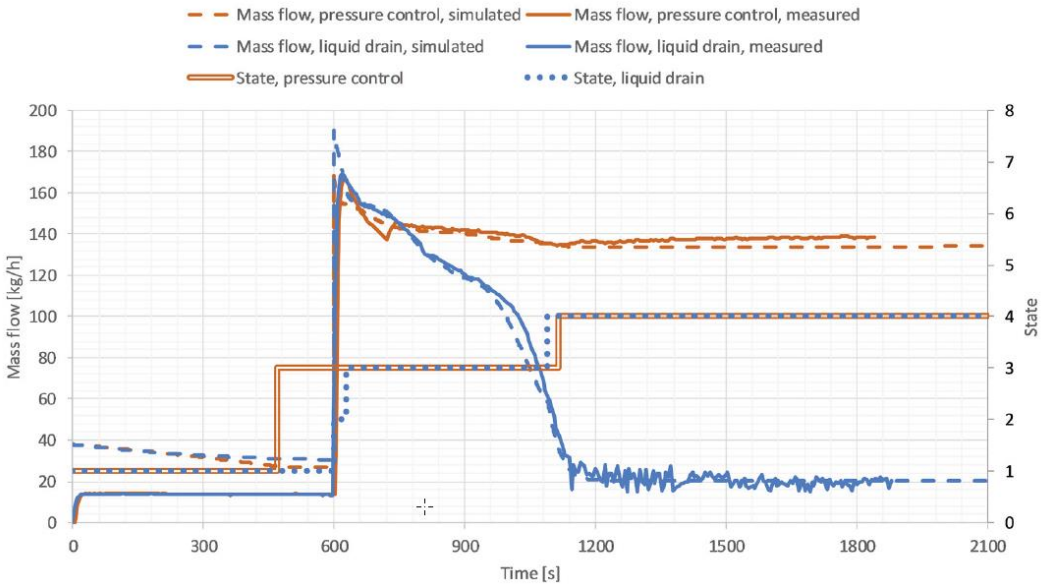

Figure 13: Measured and simulated mass flow rates

The simulations also indicate that the LD method needs more time to heat up the evaporator, but less time to complete the defrost. This observation can be related to the different pressure levels in the evaporator and the accompanying change in saturation temperature.

To further investigate the behaviour at the beginning of the filling period, the two-step solenoid valve is replaced with a slow-opening motor valve. The results presented in Figure 14 seem to indicate the model captures the behaviour better than for the abrupt opening.

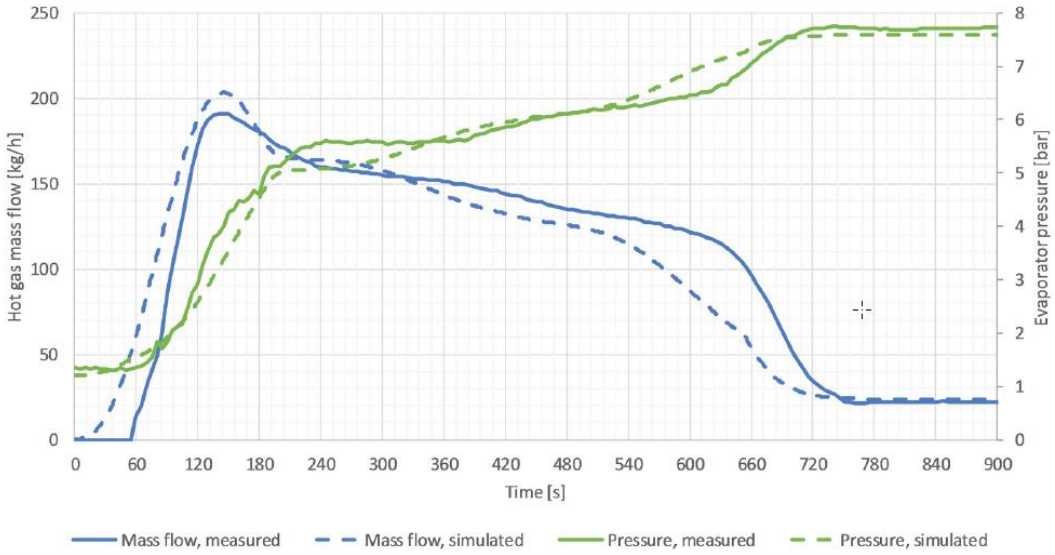

Figure 14: Measured and simulated properties for a slow-opening valve

Besides the mismatch of modelled and measured mass flow rate, there is no obvious explanation for the delayed start of the flow during the experiments. The actual opening degree of the motor valve cannot be recorded and there might be a control parameter that imposes a delay or a filter on the control signal, but that remains to be investigated.

4. Results

4.1 Energy consumption

Regardless of the employed defrost method, a certain amount of uncondensed gas passes through the evaporator. This mass flow is regarded as the main source for losses since it does not contribute much to the defrost process since the potential of the heat of the condensation cannot be exploited. The throttling process reduces the pressure of this gas flow and makes it practically equal to a hot gas bypass flow. There are also other loss mechanisms shown in Figure 15 and the definition of the categories shall be given below.

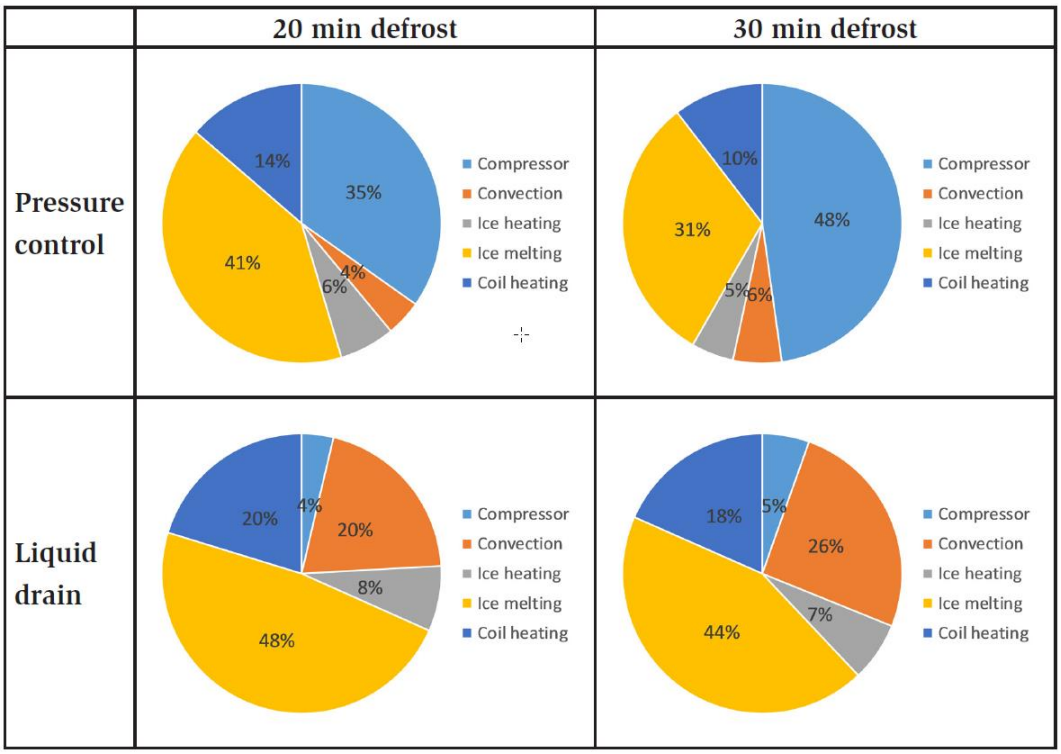

Figure 15: Energy consumption distribution comparisons

The energy used by the compressor relates to the uncondensed hot gas and is calculated with a constant isentropic efficiency of 0.7. The convective losses are sum of the energy exchange with the cold room. The contribution is negative in the beginning since the ice is colder than its surroundings, but it increases gradually with the ice and coil temperature. The additional energy needed to remove this heat from the cold room is not included. The sensible heat required to warm the ice is shown as “ice heating” in the pie charts. Here, the initial temperature and the mass of the ice are selected to match the experimental campaign and they are the same for the PC and the LD calculations. The latent heat to melt the ice is also constant for all cases due to the reasons stated above. Depending on the final coil temperature, a variable share of the energy is used to heat the metal of the evaporator after the ice has been removed. Additional energy consumption associated with the subsequent cooling of the warm coil has not been included.

Since ice heating and ice melting are the purpose of the defrost operation, these two constant contributions cannot be regarded as wasted energy while all other categories could be classified as loss. The large mass flow of uncondensed gas through the PC valve leads to a larger contribution of the recompression losses for this method.

Energy consumption	20 min defrost	30 min defrost
Pressure control	9.5 kWh	12.5 kWh
Liquid drain	8.1 kWh	8.9 kWh

The table presented above summarizes the total energy consumption that forms the basis for the diagrams in Figure 15. The two columns in the table show the results for different defrost durations and it becomes obvious that the PC method consumes much more energy for longer defrost times as the gas flow remains almost constant after the ice has been removed from the evaporator. The LD method can be regarded as partly self-regulating since the increased pressure at the end of the defrost operation leads to a very small mass flow rate and a smaller increase in energy consumption for longer defrost times. This leads to an increasing difference in energy consumption for longer defrost durations, the energy savings associated with the LD method increase from 15% to almost 30% when the defrost time is changed from 20 min to 30 min.

4.2 Refrigerant hold-up

The PC valve does not control the amount of liquid generated in the evaporator and can lead to larger amounts of refrigerant inside the evaporator. For a typical defrost cycle, Figure 16 compares the amount of refrigerant in the evaporator for the LD and the PC method.

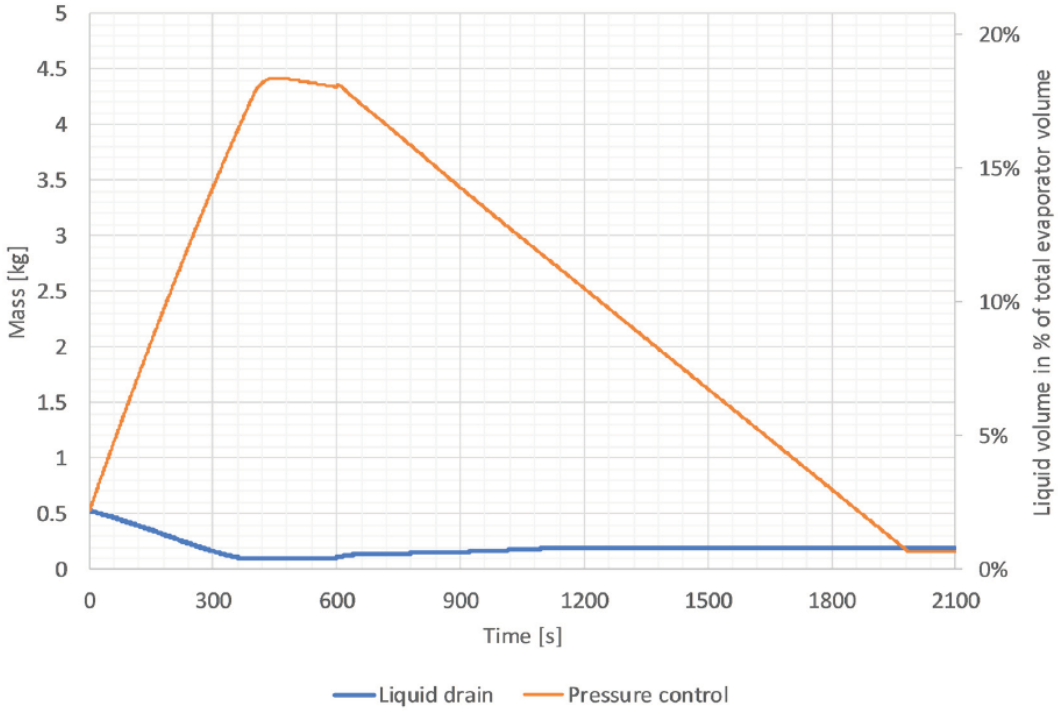

Figure 16: Simulated mass of refrigerant in the evaporator

The mass build-up in the PC cycle peaks at about 18% of the evaporator volume equalling almost 4.5 kg of ammonia. The figure illustrates that the increased defrost performance of the LD system may be related to a larger free heat transfer area in the LD system. Furthermore, the LD cycle seems to be better suited for low charge ammonia systems.

4.3 Hot gas pressure

The hot gas pressure controls the maximum condensation temperature and there is a savings potential related to a minimization of the pressure required to run a defrost system. However, there is a trade-off between low hot gas saturation temperature and long defrost times and Figure 17 shows the impact of low hot gas pressure.

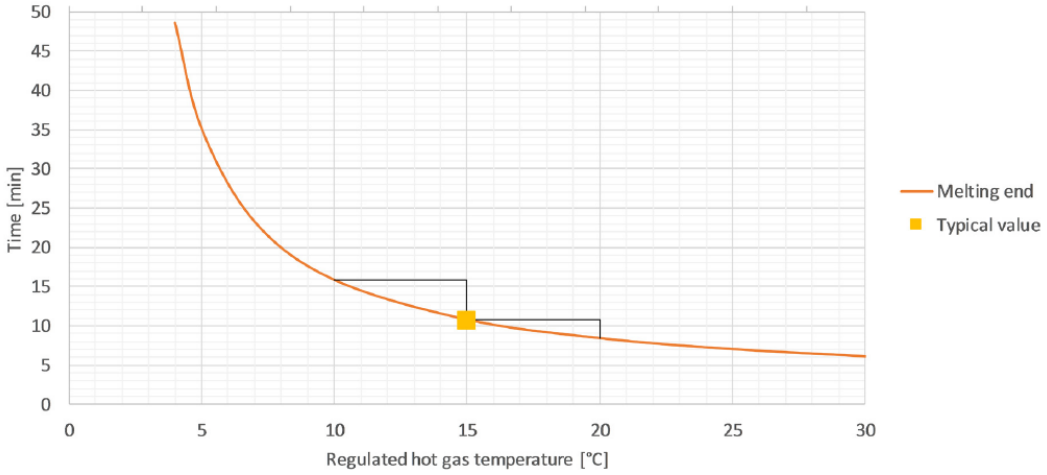

Figure 17: Defrost time versus hot gas saturation condition

For the LD method, the required defrost time increases exponentially as the hot gas saturation temperature approaches the melting temperature of the ice. For the investigated case, it takes 11 min to remove the ice at 15 °C saturation temperature, while a decrease in temperature by 5 K yields an increase in defrost time by 5 min and an increase in temperature by 5 K leads to a decrease in required defrost time by 2 min.

To analyse the savings potential associated with a reduction of the hot gas pressure, a calculation of a blast freezing tunnel in an abattoir is carried out. This case matches an existing installation with a cooling load of 1.5 MW at an evaporator temperature of -35 °C. In this example, the condenser pressure has lower limit of 25 °C due to the hot gas production requirements. The two-stage ammonia system has an open intercooler running at -10 °C. To simulate the hot gas consumption, an additional load of 200 kW is introduced at intercooler temperature. The hot gas demand is regarded as continuous because there are multiple evaporators and the selected average load matches the mean demand for running the implemented defrost schedule. Without modifying the hot gas demand, running with a floating condenser pressure of 20 °C, 15 °C and 10 °C leads to annual energy savings of 5.7%, 8.8% and 9.8%, respectively. For details, please refer to the Pack Calculation Pro report in the appendix.

Since the actual selection of the hot gas pressure also includes a buffer for flow losses and a security margin for the maximum defrost time, there is no global optimum, but the defrost simulation and the annual calculation illustrate how the hot gas pressure affect the defrost time and the energy consumption.

5. Conclusions

Hot gas-driven defrost solutions are the most popular choice for industrial refrigeration systems today. They perform well in terms of reliability, energy consumption and defrost time. Furthermore, hot gas defrost systems can be realised for all common evaporator types. However, the control of the defrost has to be designed carefully to avoid unnecessary penalties, especially regarding the energy bill.

A simple way to run a reliable and fast defrost process is by controlling the evaporator pressure during defrost. This project has shown that this well-established control method can lead to increased hot gas consumption causing high compressor loads and energy use. This effect gets amplified if the defrost cycle is not terminated in a timely manner.

Controlling the amount of liquid in the evaporator with a float valve, on the other hand, has proven to be more efficient. This method is also less prone to losses caused by inaccurate timing since it can be regarded as partly self-regulating. This method also reduces the amount of refrigerant that is present inside the evaporator and is thus a good choice for low charge systems.

For the investigated evaporator, a hot gas pressure that allows the refrigerant to condense at 15 °C seems to be a good compromise between defrost time and energy used for hot gas production.

6. References

Kristófersson, J. (2017). Måling af energiforbrug ved varmgasafrimning. *DKVF Temamøde "Varmgasafrimning".* Kolding: Dansk Køle- & Varmepumpeforening.

Kristófersson, J., Reinholdt, L., Vestergaard, N., Skovrup, M. J., Wronski, J., & Pachai, A. (2018). Defrost Efficiency for Ammonia Evaporator Systems. *Proceedings of the 13th IIR Gustav Lorentzen Conference on Natural Refrigerants.* Valencia, Spain: International Institute of Refrigeration.

Skovrup, M. J., Wronski, J., Vestergaard, N., Kristófersson, J., Reinholdt, L., & Pachai, A. (2017). Energy Savings Comparing Pressure Controlled and Liquid Drain Controlled Hot Gas Defrost. *Proceedings of the 7th Conference on Ammonia and CO2 Refrigeration Technologies.* Ohrid, Macedonia: International Institute of Refrigeration.

Vestergaard, N. (2017). *Danfoss White Paper: Effective and cost-efficient hot gas defrost methods - DKRCI.PE.FT0.A1.02.* Danfoss.

Vestergaard, N. (2017). Varmgasafrimning i industrielle anlæg - metoder og dimensionering. *DKVF Temamøde "Varmgasafrimning".* Kolding, Denmark: Dansk Køle- & Varmepumpeforening.

Vestergaard, N., & Mikhailov, A. (2016). Analysis of various ammonia defrosting systems. *Proceedings of the 12th IIR Gustav Lorentzen Conference on Natural Refrigerants.* Edinburgh, United Kingdom: International Institute of Refrigeration.

Vestergaard, N., & Skovrup, M. J. (2018). Energy and Function Analysis of Hot Gas Defrost. *Technical Papers of the 40th Annual Meeting.* Colorado Springs, Colorado, USA: International Institute of Ammonia Refrigeration.

Vestergaard, N., Kristofersson, J., Skovrup, M. J., Reinholdt, L., Wronski, J., & Pachai, A. (2017). Design requirements for effective ammonia defrost systems. *Proceedings of the 7th Conference on Ammonia and CO2 Refrigeration Technologies.* Ohrid, Macedonia: International Institute of Refrigeration.

Wronski, J. (2017). Energy Savings for Different Defrost Methods. *DKVF Temamøde "Varmgasafrimning".* Kolding: Dansk Køle- & Varmepumpeforening.